

## Different Intermediate Populations Formed by Tazobactam, Sulbactam, and Clavulanate Reacting with SHV-1 $\beta$ -Lactamases: Raman Crystallographic Evidence<sup>†</sup>

Matthew Kalp,<sup>‡</sup> Monica A. Totir,<sup>‡</sup> John D. Buynak,<sup>§</sup> and Paul R. Carey\*<sup>‡</sup>

Department of Biochemistry, Case Western Reserve University, 10900 Euclid Avenue, Cleveland, Ohio 44106, and Department of Chemistry, Southern Methodist University, P.O. Box 750314, Dallas, Texas 75275-0314

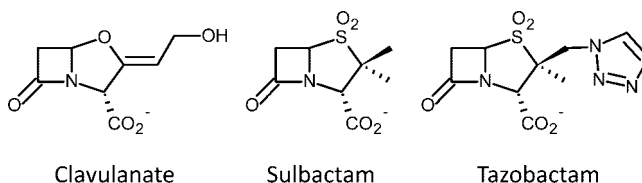
Received October 27, 2008; E-mail: paul.carey@case.edu

**Abstract:** Tazobactam, sulbactam, and clavulanic acid are the only  $\beta$ -lactamase inhibitors in clinical use. Comparative inhibitory activities of clavulanic acid, sulbactam, and tazobactam against clinically important  $\beta$ -lactamases conclude that tazobactam is superior to both clavulanic acid and sulbactam. Thus far, the majority of explanations for this phenomenon have relied on kinetic studies, which report differences in the ligands' apparent dissociation constants and number of turnovers before inactivation. Due their innate limitations, these investigations do not examine the identity of intermediates on the reaction pathway and relate them to the efficacy of the inhibitors. In the present study, the reactions between the three inhibitors and SHV-1  $\beta$ -lactamase have been examined in single crystals using a Raman microscope. The results show that tazobactam forms a predominant population of *trans*-enamine, a chemically inert species, with SHV-1, while clavulanate and sulbactam form a mixture of *trans*-enamine and two labile species, the *cis*-enamine and imine. The same reactions are then reexamined using a deacylation-deficient variant, SHV E166A, that has been used to trap acyl-enzyme intermediates for X-ray crystallographic analysis. Our Raman data show that significant differences exist between the wild-type and SHV E166A acyl-enzyme populations. Namely, compared to SHV-1, sulbactam shows significantly smaller populations of *cis*-enamine and imine in the E166A variant, while clavulanate exists almost exclusively as *trans*-enamine in the E166A active site. Using clavulanate as an example, we also show that Raman crystallography can provide novel information on the presence of multiple conformers or tautomers for intermediates within a complex reaction pathway. These insights caution against the interpretation of experimental data obtained with deacylation-deficient  $\beta$ -lactamases to make mechanistic conclusions about inhibitors within the enzyme.

### Introduction

$\beta$ -Lactamase production is the most common mechanism by which Gram-negative bacteria become resistant to  $\beta$ -lactam antibiotics such as penicillins and cephalosporins.<sup>1,2</sup> TEM-1 and SHV-1 share 68% sequence identity and are the most commonly encountered class A  $\beta$ -lactamases in Gram-negative bacteria.<sup>3</sup> Up to 90% of ampicillin resistance in *Escherichia coli* is due to the production of TEM-1, whereas SHV-1 is responsible for up to 20% of the plasmid-mediated ampicillin resistance in *Klebsiella pneumoniae*.<sup>1</sup> Thus, in present day clinical practice, bacterial infections are often treated with two drugs, one such

**Chart 1.** Schematic Diagram of the Mechanism-Based Inhibitors Clavulanate, Sulbactam, and Tazobactam



as penicillin to inhibit bacterial cell wall growth and the second (see, for example, Chart 1) to inhibit the  $\beta$ -lactamases produced by the bacteria, thereby blocking penicillin hydrolysis.<sup>2</sup> Currently, four classes of  $\beta$ -lactamase enzymes have been described. The Ambler class A, C, and D enzymes are serine hydrolases, with the fourth class being metalloenzymes.<sup>4–7</sup> The serine  $\beta$ -lactamases share a mechanism whereby their active-site serine attacks the carbonyl carbon of the  $\beta$ -lactam ring of the inhibitors shown in Chart 1 to form an acyl-enzyme complex (Scheme

<sup>†</sup> Abbreviations: TEM, class A  $\beta$ -lactamase of *Escherichia coli* first described in a Greek patient, with the name being derived from the patient's name; SHV, class A  $\beta$ -lactamase of *Klebsiella pneumoniae* initially thought to be a "sulfhydryl variant" of the TEM enzyme; HEPES, *N*-(2-hydroxyethyl)piperazine-*N'*-2-ethanesulfonic acid; HPLC, high-performance liquid chromatography; DFT, density functional theory; B3LYP, Becke, three-parameter, Lee–Yang–Parr; HF, Hartree–Fock.

<sup>‡</sup> Case Western Reserve University.

<sup>§</sup> Southern Methodist University.

(1) Bradford, P. A. *Clin. Microbiol. Rev.* **2001**, *14* (4), 933–51, Table of Contents.

(2) Helfand, M. S.; Bonomo, R. A. *Curr. Drug Targets: Infect. Disord.* **2003**, *3* (1), 9–23.

(3) Kuzin, A. P.; Nukaga, M.; Nukaga, Y.; Hujer, A. M.; Bonomo, R. A.; Knox, J. R. *Biochemistry* **1999**, *38* (18), 5720–7.

(4) Ambler, R. P. *Philos. Trans. R. Soc. London, B* **1980**, 289 (1036), 321–31.

(5) Hall, B. G.; Barlow, M. *J. Mol. Evol.* **2003**, *57* (3), 255–60.

(6) Hall, B. G.; Barlow, M. *Drug Resist. Updates* **2004**, *7* (2), 111–23.

(7) Hall, B. G.; Barlow, M. *J. Antimicrob. Chemother.* **2005**, *55* (6), 1050–1.



Previous Raman data showed that all three inhibitors formed a predominant population of the *trans*-enamine species using the deacylation-deficient mutant E166A.<sup>17–19</sup> Class A  $\beta$ -lactamases utilize an invariant glutamic acid residue, E166, to activate a water molecule for nucleophilic attack on the acyl-enzyme.<sup>20,21</sup> An aliphatic residue, such as alanine, cannot activate this water molecule and prevents regeneration of active enzyme by blocking hydrolysis of species **1**, **2**, and **3**.<sup>22–24</sup> For the E166A mutant, the accumulation of reaction intermediates in the active site, particularly the *trans*-enamine species, facilitates their detection by Raman difference spectroscopy and analysis by X-ray crystallography.<sup>17–19</sup> However, characterization of the reaction between wild-type SHV-1 and mechanism-based inhibitors proves challenging due to an increased deacylation rate constant, decreased acyl-enzyme populations, and the presence of reaction intermediates other than the *trans*-enamine. Monitoring the nature of the intermediates, their relative populations, and their time courses of formation and disappearance provides insight into the key steps in  $\beta$ -lactamase inhibition and the effect of enzyme mutations on the formation of these intermediates.<sup>25,26</sup> TEM and SHV enzymes often contain single-point mutations that confer resistance to  $\beta$ -lactamase inhibitors.<sup>23,27</sup> In the TEM family, clinical mutants containing M69I, M69L, M69V, R244S, and S130G mutations have been reported. In SHV, clinical mutants containing the M69I and S130G mutations have been isolated. Because resistance is directly related to the composition of intermediates formed between inhibitor and  $\beta$ -lactamase, a detailed study of these reaction mechanisms is warranted.

Here we present steady-state Raman difference spectra of acyl-enzyme-derived intermediates in single crystals of the  $\beta$ -lactamase enzyme. The spectra are paired with extensive quantum mechanical calculations on models for enzyme-bound intermediates that permit characterization of inhibitor degradation products, such as the imine and *cis*- and *trans*-enamine species. Two enzymes are used to acquire spectra of the acyl-enzymes: wild-type SHV-1 and SHV E166A, a deacylation-deficient laboratory mutant. X-ray structures of the *trans*-enamine acyl-enzyme of SHV E166A and the inhibitors tazobactam, sulbactam, and clavulanate have served as good starting points for the rational design of new inhibitors.<sup>18,19,28</sup> However, by comparing the difference spectra obtained with

SHV-1 and E166A, in this paper we will show that significant differences exist between the wild-type and E166A acyl-enzyme populations. Consequently, strategic drug design must take into account the identity and composition of reaction intermediates formed with the wild-type enzyme. Laboratory mutants, such as E166A, which bias the reaction pathway to trap an acyl-enzyme may provide information on intermediates that are not dominant for the wild-type enzyme and therefore may not be a reliable basis for structure-based drug design.

## Materials and Methods

**Inhibitors.** Sodium clavulanate (Smith-Kline-Beecham), sulbactam (Pfizer), and tazobactam (Wyeth Pharmaceuticals) were gifts of the respective companies. 6,6-Dideuteriosulbactam was synthesized as described in ref 15. Stock solutions (20 mM) in 2 mM HEPES buffer (pH 7.0) were prepared for use with the protein crystals.

**Protein Isolation and Purification.** The SHV-1 and E166A  $\beta$ -lactamase enzymes were isolated and purified as previously described with an additional HPLC purification step performed using a Sephadex Hi Load 26/60 column (Pharmacia, Uppsala, Sweden) and elution with phosphate-buffered saline (pH 7.4).<sup>3,17,27</sup>

**Crystallization.** SHV-1 and E166A were concentrated to 5 mg/mL in 2 mM HEPES buffer (pH 7.0) for crystallization by the vapor diffusion method using the protocol of Kuzin et al.<sup>3</sup> Briefly, the 10  $\mu$ L sitting protein drop [2 mg/mL, 0.56 mM Cymal-6 detergent (Hampton Research, Laguna Niguel, CA), 15% poly(ethylene glycol) 6000 (Hampton Research), 50 mM HEPES buffer, pH 7.0] was placed over a 0.50 mL reservoir solution containing 30% poly(ethylene glycol) and 100 mM HEPES buffer. The enzyme crystallized in approximately 1 week.

**Raman Crystallography.** The Raman microscope system has been described previously.<sup>29,30</sup> Using a cryoloop, crystals, typically 300  $\mu$ m  $\times$  300  $\mu$ m  $\times$  300  $\mu$ m in size, were transferred from the mother liquor solution to a 4  $\mu$ L drop of 2 mM HEPES. A 647 nm, 80 mW Kr<sup>+</sup> laser beam (Innova 70 C, Coherent, Palo Alto, CA) was focused on the protein crystals in a 4  $\mu$ L hanging drop using the 20 $\times$  objective of the Raman microscope. During data collection, spectra were acquired for 10 s, and 10 accumulations were averaged for each time point. After spectra of the apo- $\beta$ -lactamase protein crystals were obtained, inhibitors were added to the drop to achieve a final volume of 5  $\mu$ L and a final inhibitor concentration of 5 mM. Spectra were then acquired every 2–3 min after addition of an inhibitor. To obtain difference spectra, an apo- $\beta$ -lactamase spectrum was subtracted from the protein/inhibitor spectra at varying time intervals following addition of inhibitor. HEPES buffers in D<sub>2</sub>O were prepared using nondeuterated HEPES and titrated with NaOD to pD 6.55 (pD = pH + 0.45).<sup>31</sup> Stock solutions of inhibitors were prepared in the deuterated 2 mM HEPES buffer (pD 7.0). Protein crystals, prepared as described above, were added to a 4  $\mu$ L drop of 2 mM deuterated HEPES buffer (pD 7.0). Data collecting and processing were performed using HoloGRAMS and GRAMS/AI 7 software (ThermoGalactic, Inc., Salem, NH). Raman spectra of the inhibitors that were used were obtained under similar conditions. Spectra were obtained for 4  $\mu$ L drops of 100 mM inhibitor solutions prepared in 100 mM HEPES (pH 7.0). Low-temperature spectra were collected at 8  $^{\circ}$ C. To achieve this, the crystal was set up on a coverslip resting on a metal chamber that was connected to a low-temperature thermostatically controlled bath containing a 1:1 mixture of water and glycerin.

- (17) Helfand, M. S.; Totir, M. A.; Carey, M. P.; Hujer, A. M.; Bonomo, R. A.; Carey, P. R. *Biochemistry* **2003**, *42* (46), 13386–92.
- (18) Padayatti, P. S.; Helfand, M. S.; Totir, M. A.; Carey, M. P.; Carey, P. R.; Bonomo, R. A.; van den Akker, F. *J. Biol. Chem.* **2005**, *280* (41), 34900–7.
- (19) Padayatti, P. S.; Helfand, M. S.; Totir, M. A.; Carey, M. P.; Hujer, A. M.; Carey, P. R.; Bonomo, R. A.; van den Akker, F. *Biochemistry* **2004**, *43* (4), 843–8.
- (20) Hermann, J. C.; Ridder, L.; Holtje, H. D.; Mulholland, A. J. *Org. Biomol. Chem.* **2006**, *4* (2), 206–10.
- (21) Meroueh, S. O.; Fisher, J. F.; Schlegel, H. B.; Mobashery, S. *J. Am. Chem. Soc.* **2005**, *127* (44), 15397–407.
- (22) Escobar, W. A.; Tan, A. K.; Fink, A. L. *Biochemistry* **1991**, *30* (44), 10783–7.
- (23) Gibson, R. M.; Christensen, H.; Waley, S. G. *Biochem. J.* **1990**, *272* (3), 613–9.
- (24) Knox, J. R.; Moews, P. C.; Escobar, W. A.; Fink, A. L. *Protein Eng.* **1993**, *6* (1), 11–8.
- (25) Helfand, M. S.; Taracila, M. A.; Totir, M. A.; Bonomo, R. A.; Buynak, J. D.; van den Akker, F.; Carey, P. R. *Biochemistry* **2007**, *46* (29), 8689–99.
- (26) Totir, M. A.; Padayatti, P. S.; Helfand, M. S.; Carey, M. P.; Bonomo, R. A.; Carey, P. R.; van den Akker, F. *Biochemistry* **2006**, *45* (39), 11895–904.
- (27) Hujer, A. M.; Hujer, K. M.; Bonomo, R. A. *Biochim. Biophys. Acta* **2001**, *1547* (1), 37–50.

- (28) Padayatti, P. S.; Sheri, A.; Totir, M. A.; Helfand, M. S.; Carey, M. P.; Anderson, V. E.; Carey, P. R.; Bethel, C. R.; Bonomo, R. A.; Buynak, J. D.; van den Akker, F. *J. Am. Chem. Soc.* **2006**, *128* (40), 13235–42.
- (29) Carey, P. R. *Annu. Rev. Phys. Chem.* **2006**, *57*, 527–54.
- (30) Carey, P. R. *Chem. Rev.* **2006**, *106* (8), 3043–54.
- (31) Krezel, A.; Bal, W. *J. Inorg. Biochem.* **2004**, *98* (1), 161–166.

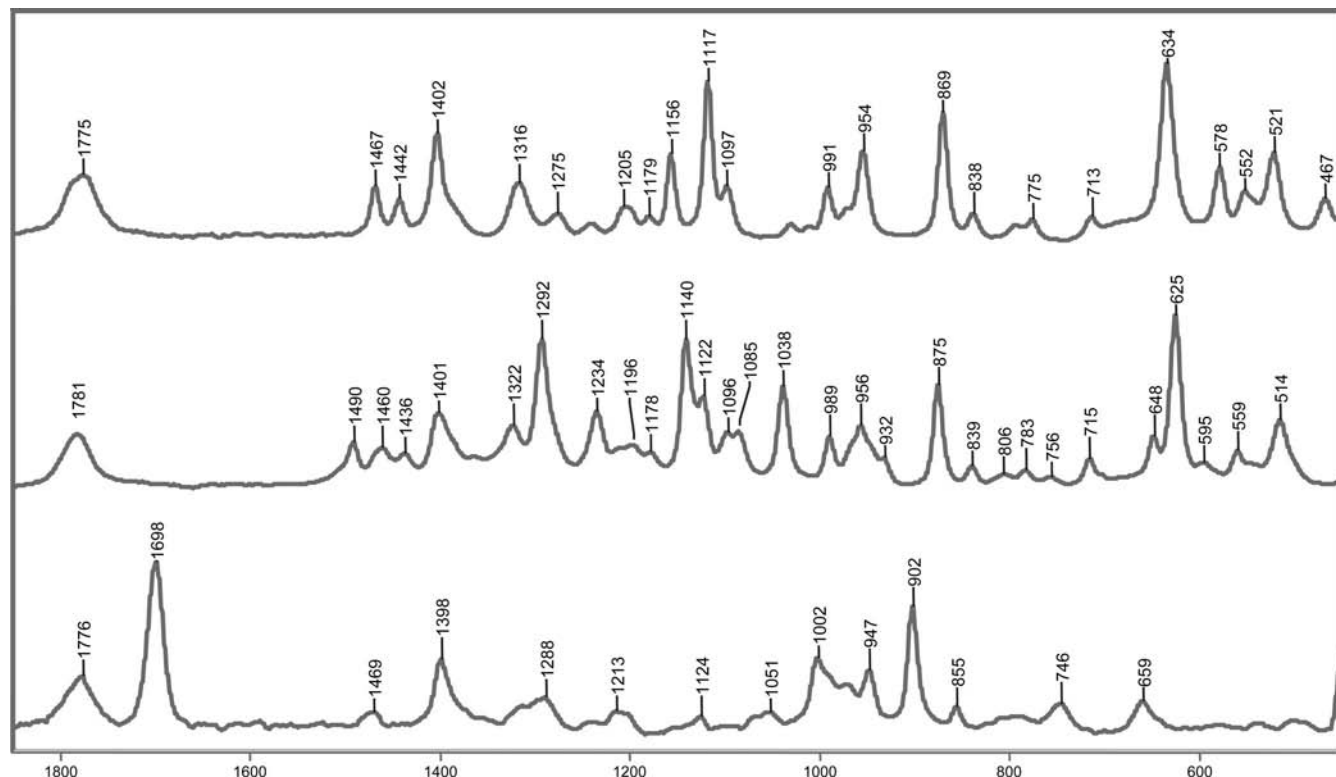


**Figure 1.** Raman spectra of subactam (top), tazobactam (middle), and clavulanate (bottom). The  $\beta$ -lactam carbonyl stretch near  $1775\text{ cm}^{-1}$  is common to the inhibitors and disappears as a result of acylation.

**Calculations.** Ab initio quantum mechanical calculations were performed to predict the Raman spectra of compounds **A–G** (see Tables 1, 3, and 4) using Gaussian 03.<sup>32</sup> Calculations were performed at the DFT level using the 6-31+G(d) basis set. DFT calculations were performed with Becke's three-parameter hybrid method using the correlation functional of Lee, Yang, and Parr (B3LYP), with 20% HF exact exchange mixing. A standard scaling factor of 0.961 was applied to the calculated values.<sup>33</sup>

## Results and Discussion

**Raman Spectra of the Inhibitors.** The Raman spectra of tazobactam, subactam, and clavulanate are shown in Figure 1. The weak band near  $1775\text{ cm}^{-1}$  corresponds to the stretch of the carbonyl in the  $\beta$ -lactam ring. Nucleophilic attack on the lactam carbonyl by the active-site S70 produces acyl-enzymes that result in the disappearance of the lactam carbonyl stretching feature. This indicates breakage of the C–N bond in the lactam ring and gives rise to a broad, weak carbonyl band between  $1720$  and  $1740\text{ cm}^{-1}$ . The latter feature is often too diffuse to be seen in the Raman spectrum. Following formation of the initial acyl-enzyme, opening of the thiazolidine ring, after departure of the sulfinate group at C5, results in the formation of an imine. In the Raman spectrum, this second ring opening leads to disappearance of the C–S stretch seen near  $630\text{ cm}^{-1}$  in the parent spectra of tazobactam and subactam. The imine rapidly partitions among three competing pathways: (1) hydrolysis, which regenerates active enzyme, (2) formation of an

S130-bound vinyl carboxylic acid species, or (3) rearrangement to a *cis*- or *trans*-enamine acyl-enzyme.

**SHV-1 Reacting with Tazobactam Predominantly Forms a *trans*-Enamine Population.** Raman difference spectra from  $1200$  to  $1800\text{ cm}^{-1}$  for  $[\text{SHV-1} + \text{tazobactam}] - [\text{SHV-1}]$  are shown in Figure 2. The region from  $1550$  to  $1800\text{ cm}^{-1}$  is critical to our discussion and contains many bands largely due to stretching modes from a number of acyl-enzyme species; these are described in detail below. In addition, the low-intensity feature near  $1678\text{ cm}^{-1}$  is assigned to protein amide I modes due to minor secondary structural changes occurring upon acylation. For the native crystals, the amide I profile,  $1620$ – $1700\text{ cm}^{-1}$ , contains contributions at different positions from modes due to  $\alpha$ -helices,  $\beta$ -sheets, and unordered regions of polypeptide. When  $\beta$ -strand features appear in the difference spectra, such as the Raman lines near  $1680\text{ cm}^{-1}$  in Figure 2, a ligand-induced conformational change involving the  $\beta$ -structure is indicated.<sup>34</sup> However, these conformational changes are small: when the intensity at  $1680\text{ cm}^{-1}$  is normalized to the parent amide I band in the apo spectrum, less than 5% of the overall amide I band intensity moves to the  $\beta$ -space. The residues giving rise to the  $\beta$ -strand features near  $1680\text{ cm}^{-1}$  are in “Ramachandran  $\beta$ -space” but lack the interstrand hydrogen bonds found in the  $\beta$ -sheet. Other major modes include  $1460\text{ cm}^{-1}$  due to protein and acyl group C–H deformations and a peak near  $1380\text{ cm}^{-1}$  due to the symmetric  $-\text{CO}_2^-$  stretch of tazobactam. The band near  $1290\text{ cm}^{-1}$  is due to the substrate's triazole moiety, while the  $1240\text{ cm}^{-1}$  feature probably contains contributions from  $-\text{N}-\text{H}$  deformation modes of the acyl group and amide III motions of the protein. The broad features centered at  $1500\text{ cm}^{-1}$

(32) Frisch, M. J.; et al. *Gaussian 03*, revision C.02; Gaussian, Inc.: Wallingford, CT, 2004.

(33) Johnson, R. D., III. *NIST Computational Chemistry Comparison and Benchmark Database*; National Institute of Standards and Technology: Gaithersburg, MD, 2006; NIST Standard Reference Database Number 101.

(34) Zheng, R.; Zheng, X.; Dong, J.; Carey, P. R. *Protein Sci.* **2004**, *13* (5), 1288–94.

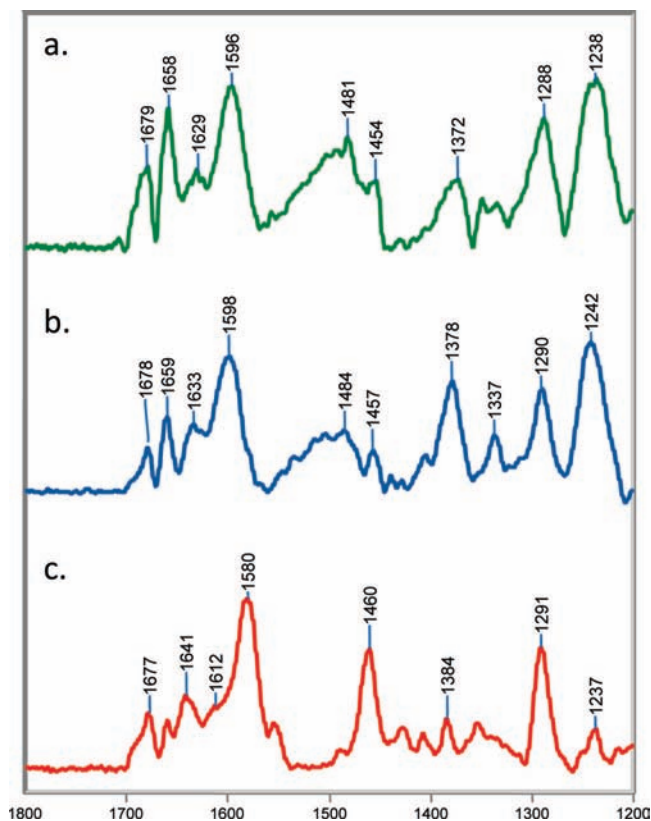


**Figure 2.** Steady-state Raman difference spectra of the acyl-enzyme-derived intermediates from tazobactam with SHV-1 in (a) H<sub>2</sub>O at room temperature, (b) H<sub>2</sub>O at 8 °C, and (c) D<sub>2</sub>O at room temperature.

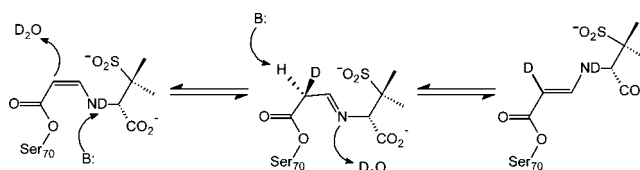
are experimental artifacts due to light scattering from the material of the crystal mounting cell.

For tazobactam in the crystal complex, the Raman difference spectra in the double bond stretching region reveal the formation of an intermediate band at 1596 cm<sup>-1</sup> in H<sub>2</sub>O and 1580 cm<sup>-1</sup> in D<sub>2</sub>O (parts a and c, respectively, of Figure 2). On the basis of previous studies with the deacylation-deficient variant SHV E166A, this feature is assigned to the *trans*-enamine.<sup>17</sup> The conjugated O=C–C=C–NH– fragment gives rise to a fairly intense Raman band that responds to NH/ND exchange in D<sub>2</sub>O. The calculated stretching frequencies for a *trans*-enamine model compound **A** and mono- and dideuterated analogues **B** and **C** are shown in Table 1. The calculated stretching frequency for *trans*-enamine **A** (1594 cm<sup>-1</sup>) agrees with the experimental result (1596 cm<sup>-1</sup>); however, replacing the amine hydrogen of **A** with deuterium (as in **B**) does not reproduce the isotope shift observed on NH/ND exchange in Figure 2c (Table 1). The difference between the experimental and observed isotope shifts suggests that *another* deuterium from the solvent is incorporated into the enamine skeleton. The imine is formed immediately after the second ring opening and rapidly equilibrates with the *cis*- and *trans*-enamine. As illustrated in Scheme 2, deuterium incorporation occurs at C6 after multiple tautomerization events between the enamine and imine species. If a deuterium is included in model compound **C** at C6, the calculated stretching frequency (1581 cm<sup>-1</sup>) now agrees with the experimental value (1580 cm<sup>-1</sup>). If deuterium incorporation at C6 were to proceed slowly in D<sub>2</sub>O, then the *trans*-enamine peak would shift from 1596 to 1580 cm<sup>-1</sup> as a function of time. However, time dependence over a period of 1–60 min was not observed, which suggests that tautomerization is rapid and deuterium incorpora-

**Table 1.** Comparison of the Theoretical and Experimental O=C–C=C–NH– Stretching Frequencies of a Model *trans*-Enamine Acyl-Enzyme and Isotopologues

O=C–C=C–N– stretch (cm <sup>-1</sup> )	<b>A</b> <i>trans</i> -enamine (–NH–)	<b>B</b> <i>trans</i> -enamine (–ND–)	<b>C</b> <i>trans</i> -enamine (–ND–, D at C6)
theoretical	1594	1590	1579
experimental	1595	–	1581

**Scheme 2.** Proposed Reaction Scheme for C6 H/D Exchange in D<sub>2</sub>O upon Enamine/Imine Tautomerization



tion at C6 is complete before 1 min. On the basis of QM calculations, the band observed at 1630 cm<sup>-1</sup> is assigned to the antisymmetric –CO<sub>2</sub><sup>-</sup> stretch coupled to the O=C–C=C–NH– stretch of the enamine backbone. As illustrated by the Raman frequency at 1612 cm<sup>-1</sup> (Figure 2c), this mode also responds to NH/ND exchange due to significant contribution from –NH– bending motions of the *trans*-enamine. The shift from 1630 to 1612 cm<sup>-1</sup> is faithfully reproduced in the calculations. Lastly, the presence of the *trans*-enamine is also supported by a band at 969 cm<sup>-1</sup>, which is assigned to the *trans*-HC=CH wag of the enamine (data not shown).

We assign the band at 1658 cm<sup>-1</sup> to a protonated imine species (Figure 2a). The strongest evidence for this comes from calculations and chemical modifications of the intermediate involving clavulanate (see below). The corresponding Raman peak for tazobactam is assigned to the C=NH<sup>+</sup> stretch of the protonated imine by analogy to clavulanate. In D<sub>2</sub>O, the hydrogen atom attached to the imine nitrogen is expected to exchange with deuterium after repeated deprotonation/protonation cycles. As anticipated, the NH/ND exchange shifts the 1658 cm<sup>-1</sup> mode to 1641 cm<sup>-1</sup> (Figure 2c). Calculations on model compounds indicate that the Raman scattering cross-section of the imine may be up to 2 times greater than the scattering cross-section of the *trans*-enamine. As such, the strong feature at 1658 cm<sup>-1</sup> only represents a minor population of imine acyl-enzymes.

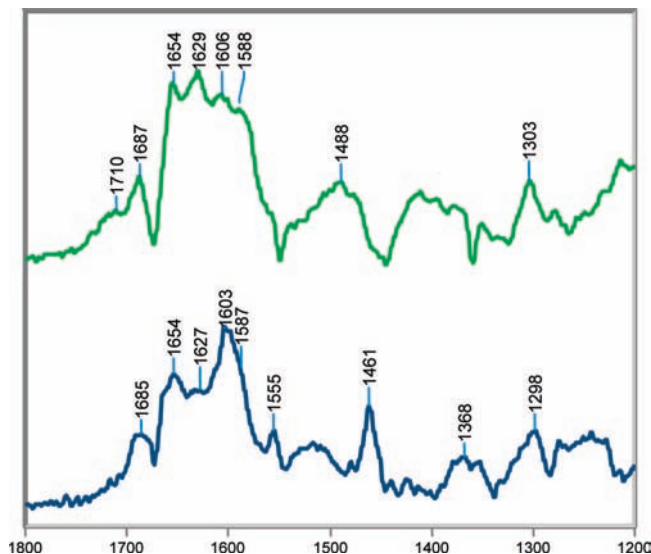
Additional insights regarding the thermodynamics of protein–ligand interactions can be obtained by comparing data collected at low and room temperature. Thus, using a simple home-built cell, the reaction between tazobactam and SHV-1 was followed in a single crystal at 8 °C. In the difference spectra at 8 °C, several ligand-derived band shapes narrow including the symmetric –CO<sub>2</sub><sup>-</sup> stretch near 1380 cm<sup>-1</sup>, the breathing mode of the triazolyl moiety near 1290 cm<sup>-1</sup>, and the *trans*-enamine peak near 1596 cm<sup>-1</sup> (Figure 2b). The change is most striking for the *trans*-enamine feature whose bandwidth at half-height

**Table 2.** Raman Peak Assignments for the Major Protein and Acyl-Enzyme Bands in the Tazobactam/SHV-1 Difference Spectra Shown in Figure 2

vibration	frequency in H <sub>2</sub> O (cm <sup>-1</sup> )	frequency in D <sub>2</sub> O (cm <sup>-1</sup> )
amide I $\beta$ -strand	1679	1678
$\nu(\text{C}=\text{NH}^+)$ of imine	1658	1641
$\nu_{\text{as}}(\text{CO}_2^-)$ coupled to $\nu(\text{O}=\text{C}-\text{C}=\text{C}-\text{NH}-)$	1629	1612 (sh)
$\nu(\text{O}=\text{C}-\text{C}=\text{C}-\text{NH}-)$ of <i>trans</i> -enamine	1596	1580
artifact	1500 (br)	
$\nu_{\text{s}}(\text{CO}_2^-)$	1372	1378
triazolyl	1288	1291
-NH- deformation of ligand and/or protein	1238	
<i>trans</i> -HC=CH wag	969	930

decreases from 34 cm<sup>-1</sup> at room temperature to 28 cm<sup>-1</sup> at 8 °C, or approximately 20% (parts a and b, respectively, of Figure 2). In Raman spectroscopy, broadened band shapes often result from conformational heterogeneity.<sup>18</sup> The broader widths of the tazobactam-derived bands at room temperature are ascribed to the existence of a range of close-lying conformations. Essentially, these have the parent *trans*-enamine structure found in the tazobactam complex; however, dynamic excursions about the observed mean torsional angles lead to line broadening of the main feature near 1596 cm<sup>-1</sup>. A crystal structure of the SHV E166A/tazobactam complex revealed the inhibitor covalently bound in the *trans*-enamine intermediate state with close to 100% occupancy in the active site. The covalently bound tazobactam participates in a number of interactions with the protein: (1) The inhibitor's carboxylate moiety forms a 2.7 Å hydrogen bond with the N $\delta$ 2 atom of N132. (2) The tazobactam triazolyl moiety's N17 nitrogen atom makes a 2.7 Å hydrogen bond with a water, which is involved in additional interactions with K234 and S130. (3) In addition to this hydrogen bond, the triazolyl moiety is also involved in hydrophobic interactions with Y105.<sup>19</sup> It is assumed that the *trans*-enamine conformation observed by X-ray crystallography is thermodynamically stable and that the aforementioned protein–ligand interactions (e.g., van der Waals, hydrophobic, hydrogen bonds, etc.) contribute to its enthalpic stabilization. Lowering the temperature selects for the lowest energy *trans*-enamine conformations, i.e., having the optimal protein–ligand interactions. In the Raman spectrum, these contributions are reflected by narrower band shapes, especially for functional groups that participate in these key interactions, such as the carboxylate and triazole moieties.

Lastly, the triazole moiety of tazobactam serves as an internal intensity standard to assess the relative contribution of a particular intermediate to the total acyl-enzyme population. This is accomplished by determining the signal ratio of the main triazole mode at 1290 cm<sup>-1</sup> to the respective enamine or imine mode. For example, a crystal structure of SHV E166A with tazobactam revealed a covalently bound *trans*-enamine intermediate with close to 100% occupancy.<sup>19</sup> In the Raman spectrum of the tazobactam/SHV E166A complex, the ratio of the intensities of the *trans*-enamine peak to the triazole peak ( $I_{1595}/I_{1290}$ ) is 1.60 (Supporting Information Figure 1). In the difference spectrum between the wild-type enzyme and tazobactam,  $I_{1595}/I_{1290}$  is 1.25 (Figure 2a). This signifies that the wild-type enzyme forms slightly less of the *trans*-enamine intermediate with tazobactam than E166A, which forms a stoichiometric *trans*-enamine intermediate. The remainder of the acyl-enzyme population for the wild-type enzyme is attributed to the imine. As predicted from the X-ray data, the 1658 cm<sup>-1</sup> band of the imine is absent in the E166A difference spectrum with tazobactam (Supporting Information Figure 1). We conclude that

**Figure 3.** Steady-state Raman difference spectra of the acyl-enzyme-derived intermediates from sulbactam with SHV-1 (top) and SHV E166A (bottom) in H<sub>2</sub>O at room temperature.

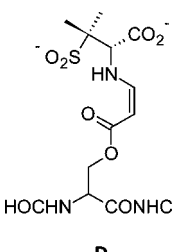
with wild-type SHV-1 tazobactam forms an acyl-enzyme population dominated by the *trans*-enamine but which does have a minor contribution from the imine. The major peaks in the spectrum are assigned in Table 2.

**SHV-1 Reacting with Sulbactam Forms a Mixture of Acyl-Enzymes.** Sulbactam is another inhibitor of serine  $\beta$ -lactamases and is normally partnered with the common penicillin-based antibiotic ampicillin. In a previous account, it was suggested that sulbactam was a poorer inactivator than tazobactam because it formed less *trans*-enamine with the deacylation-deficient E166A enzyme.<sup>17</sup> The Raman spectra in this section confirm this but now show that wild-type SHV-1 forms even greater populations of *cis*-enamine and imine.

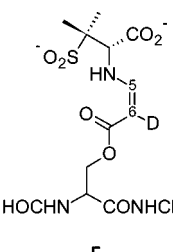
Difference spectra between sulbactam and SHV-1 (top) or SHV E166A (bottom) are shown in Figure 3. With the wild-type enzyme, it is immediately obvious that sulbactam, unlike tazobactam, does not form a predominant population of *trans*-enamine. The conjugated O=C–C=C–NH– stretch of the *trans*-enamine at 1606 cm<sup>-1</sup> is up-shifted by 10 cm<sup>-1</sup> compared to tazobactam. While the parent *trans*-enamine structure of sulbactam is chemically identical to tazobactam, the torsional angles in the O=C–C=C–NH– fragment are slightly different from those for the tazo-derived fragment, accounting, in part, for the differences in the position of the stretching feature.<sup>18</sup> A peak of similar intensity at 1588 cm<sup>-1</sup> is assigned to the O=C–C=C–NH– stretch of the *cis*-enamine. The most compelling evidence for this assignment comes from combined X-ray and Raman crystallographic studies on the intermediates formed between SHV S130G, an inhibitor-resistant  $\beta$ -lactamase, and tazobactam. By X-ray analysis, an electron density consistent with a *cis*-enamine was found in the active site.<sup>35</sup> When the same complex was subject to Raman analysis, a prominent peak at 1585 cm<sup>-1</sup> was present in the difference spectrum (Supporting Information Figure 1). While the agreement between the X-ray and Raman data alone allows us to confidently assign the 1585 cm<sup>-1</sup> signature to the C=C stretch of the *cis*-enamine, the assignment is additionally supported by two other factors:

(35) Sun, T.; Bethel, C. R.; Bonomo, R. A.; Knox, J. R. *Biochemistry* **2004**, *43* (44), 14111–7.

**Table 3.** Comparison of the Theoretical and Experimental  $\text{O}=\text{C}-\text{C}=\text{C}-\text{NH}-$  Stretching Frequencies of a Model *cis*-Enamine Acyl-Enzyme and Isotopologue



**D**



**E**

$\text{O}=\text{C}-\text{C}=\text{C}-\text{N}-$ stretch ( $\text{cm}^{-1}$ )	<b>D</b> <i>cis</i> -enamine ( <i>s-cis</i> )	<b>E</b> <i>cis</i> -enamine (D at C6)
theoretical	1585	1579
experimental	1588	1581

(a) in simple model olefins, the *cis*-isomer has its  $\text{C}=\text{C}$  stretch about  $20 \text{ cm}^{-1}$  below the signature for the *trans*-isomer,<sup>36</sup> and (b) calculations for the *cis*-enamine, as in compound **D** (Table 3), reveal good agreement for the major feature near  $1588 \text{ cm}^{-1}$ . Thus, for wild-type SHV-1, the main assignments in the double bond region are (i)  $1588 \text{ cm}^{-1}$ , *cis*-enamine, (ii)  $1606 \text{ cm}^{-1}$ , *trans*-enamine, (iii)  $1629 \text{ cm}^{-1}$ , asymmetric  $-\text{CO}_2^-$  stretch coupled to an enamine skeletal stretch, and (iv)  $1654 \text{ cm}^{-1}$ , protonated imine. Therefore, unlike tazobactam, significant populations of imine and *cis*-enamine coexist with the *trans*-enamine. In the difference spectra with E166A, the Raman data show that sulbactam forms a *trans*-enamine acyl-enzyme that exhibits a relatively intense band near  $1603 \text{ cm}^{-1}$  due to a stretching motion of the  $\text{O}=\text{C}-\text{C}=\text{C}-\text{NH}-$ . The asymmetry of this main band profile suggests the presence of a feature near  $1587 \text{ cm}^{-1}$ , which likely results from the  $\text{O}=\text{C}-\text{C}=\text{C}-\text{NH}-$  stretch of a small population of *cis*-enamine (Figure 3, bottom). The *cis/trans*-enamine vibrations couple with the asymmetric  $-\text{CO}_2^-$  stretch to give an unresolved medium-intensity band near  $1630 \text{ cm}^{-1}$ . Lastly, the  $1655 \text{ cm}^{-1}$  band is assigned to the  $\text{C}=\text{NH}^+$  stretch of the imine acyl-enzyme. The assignment of the *trans*-enamine's major Raman mode is reported in ref 17; however, in the present study, an upgraded Raman cell was used to collect the spectra. This latest cell results in an increased signal-to-noise ratio and better resolution of the complex double bond stretching region. As a result, we are able to confidently assign vibrations of the *cis*-enamine and imine and extend our previous work. Thus, with sulbactam, both E166A and SHV-1 show evidence for *trans*- and *cis*-enamine and an imine population. However, for E166A, the *trans*-enamine population appears to predominate.

Further insight is provided by following the reaction with 6,6-dideuteriosulbactam. The difference spectrum of 6,6-dideuteriosulbactam reacting with SHV-1 after 15 min is shown in Figure 4a. The spectrum is similar to that obtained with sulbactam; however, the positions of key peaks in the double bond region are down-shifted due to isotopic substitution at C6. Additionally, the data (shown at 15, 60, and 90 min in parts a, b, and c, respectively, of Figure 4) are time-dependent due to the effect of isotope scrambling with the water solvent. We assign the feature at  $1581 \text{ cm}^{-1}$  to a deuterated *cis*-enamine (E,

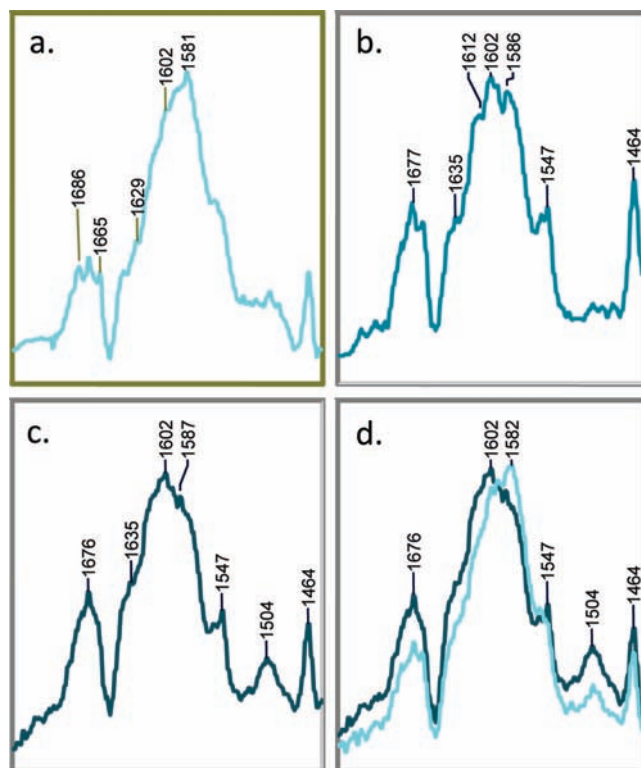


**Figure 4.** Partial Raman difference spectra of the acyl-enzyme-derived intermediates from dideuteriosulbactam with SHV-1 in  $\text{H}_2\text{O}$  at room temperature at (a) 10 min, (b) 60 min, and (c) 90 min. The spectra at 10 and 90 min are superimposed in panel d.

Table 3). In the vibrational spectrum obtained with unlabeled sulbactam, the *cis*- $\text{O}=\text{C}-\text{C}=\text{C}-\text{NH}-$  group gives rise to a strong feature near  $1588 \text{ cm}^{-1}$  (Figure 3). Thus, we anticipated that this stretch down-shifts to  $1581 \text{ cm}^{-1}$  when the compound is deuterated at C6. QM calculations on deuterated *cis*-enamine **E** support this assignment and predict a strong stretching vibration near  $1579 \text{ cm}^{-1}$  (Table 3). As was the case with tazobactam, D/H exchange with the solvent results in protium incorporation at C6 after multiple tautomerization events between the enamine and imine species (Scheme 2). This phenomenon is apparent when we compare the 6,6-dideuteriosulbactam spectra at 15 and 60 min (parts a and b, respectively, of Figure 4). In these spectra, D/H exchange results in movement of the *cis*-enamine's  $\text{O}=\text{C}-\text{C}=\text{C}-\text{NH}-$  stretch from  $1581 \text{ cm}^{-1}$  at 15 min to  $1586 \text{ cm}^{-1}$  at 60 min. Note that the *cis*-enamine frequency at 60 and 90 min (Figure 4b,c) with dideuteriosulbactam is the same as that obtained with unlabeled sulbactam. This is further confirmation that exchange at C6, although slow, is complete. The peak for the *trans*-enamine is unresolved in the  $1600 \text{ cm}^{-1}$  region at 15 min (Figure 4a) but gains intensity throughout the reaction. At 60 min, the intensity of the *trans* form is equal to that of the *cis* form, and at 90 min, the *trans* stretch at  $1602 \text{ cm}^{-1}$  is the dominant feature of the spectrum and appears at initially the same position as that for isotopically unlabeled sulbactam (Figure 3a).

From the data presented in this section, we offer two hypotheses explaining why sulbactam is a less effective inhibitor of SHV-1 than tazobactam: (1) it forms *absolutely* less *trans*-enamine with the  $\beta$ -lactamase, and (2) it forms *relatively* more of the other reaction intermediates, such as the *cis*-enamine and deacylation-prone imine. The only difference between sulbactam

(36) Daimay, L.-V. C.; Norman, B.; Fateley, W. G.; Grasselli, J. G. *The Handbook of Infrared and Raman Characteristic Frequencies of Organic Molecules*; Academic Press, Inc.: Boston, 1991; p 501.

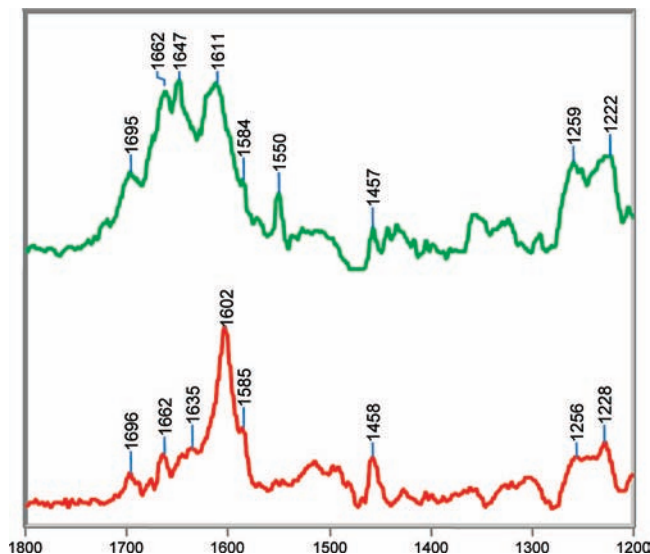


**Figure 5.** Steady-state Raman difference spectra of the acyl-enzyme-derived intermediates from clavulanate with SHV-1 (top) or SHV E166A (bottom) in H<sub>2</sub>O at room temperature.

and tazobactam is the presence of a triazolyl moiety on the C2  $\beta$ -methyl group of the latter. There are two possible explanations as to how the triazolyl group might favor formation of the *trans*-enamine: (1) rotation of the imine intermediate about the C5–C6 bond is faster in the case of tazobactam than it is when the triazole is absent, as in sulbactam, probably due to some steric clashes in the active site, and (2) once the *trans*-enamine of tazobactam is formed, it is stabilized via interactions between the triazole ring and the protein.<sup>19</sup> While these explanations are not mutually exclusive, one thing is clear: removing the triazole group results in an inferior inhibitor.

**Clavulanic Acid Predominantly Forms a *trans*-Enamine with the E166A Mutant but an Imine with SHV-1.** In the previous section, we showed that the acyl-enzymes formed between E166A and sulbactam consist predominantly of *trans*-enamine with minor populations of *cis*-enamine and imine. The same species occur in the acyl-enzymes formed by wild-type SHV-1 except that the relative populations of *cis*-enamine and imine increase significantly (Figure 3). The findings with clavulanic acid are even more striking since the spectra for the E166A intermediates reveal an overwhelming population of *trans*-enamine, with, at best, minimal populations of *cis*-enamine and imine, whereas in the wild-type enzyme greatly increased populations of imine bring about profound spectral changes (Figure 5). Discussions in the literature emphasize that clavulanic acid and the sulfones inhibit  $\beta$ -lactamases by a similar mechanism. However, the Raman difference analysis emphasizes important mechanistic differences between clavulanate and the sulfones. The spectrum of the clavulanate/SHV E166A complex is shown in Figure 5 (bottom). The Raman line at 1602 cm<sup>-1</sup> marks the presence of a predominant population of *trans*-enamine. This finding is in agreement with an inhibitor-bound X-ray structure of E166A, which also revealed a linear *trans*-enamine covalently attached to S70.<sup>18</sup> Moreover, both the Raman data and X-ray omit density maps indicate that the *trans*-enamine intermediate is decarboxylated. This is evidenced in the Raman spectrum as an absence in the intensity of the  $-\text{CO}_2^-$  symmetric stretch near 1400 cm<sup>-1</sup> and the coupled  $-\text{CO}_2^-$  antisymmetric stretch near 1630 cm<sup>-1</sup> (see Table 2 for assignments).<sup>17,18</sup> A similar decarboxylated *trans*-enamine

**Table 4.** Comparison of the Theoretical and Experimental C=NH<sup>+</sup> Stretching Frequencies of Two Tautomeric Imines of Clavulanate

**F**

**G**

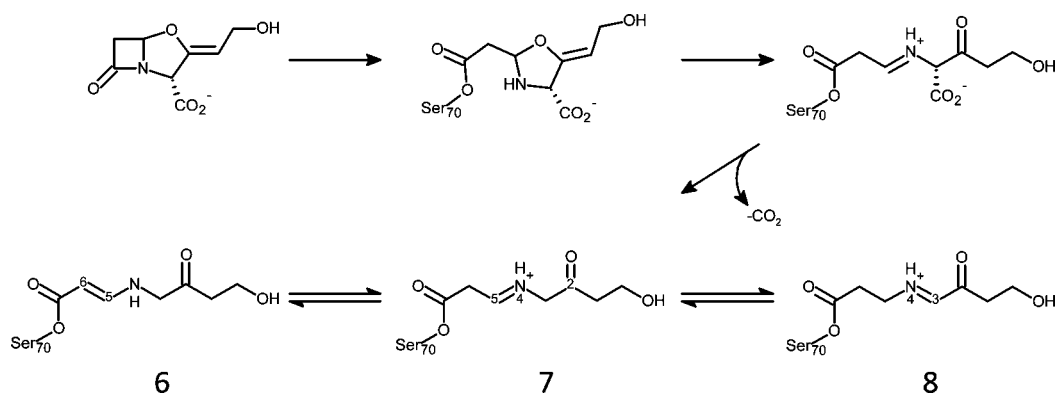
C=NH <sup>+</sup> stretch (cm <sup>-1</sup> )	F protonated imine	G protonated imine
theoretical	1663	1648
experimental	1658	1649

intermediate is made by clavulanate with wild-type SHV-1; however, its precise conformation and relative population in the SHV-1 active site differ from those of E166A. The frequency of the *trans*-enamine stretch in the wild type is increased by 10 cm<sup>-1</sup>. The O=C–C=C–NH– stretching frequency is dependent on the O–C–C–C dihedral angle; thus, the conformation of the linear *trans*-enamine must vary between E166A and the wild type, which leads to minor frequency differences.<sup>17–19</sup> To assess the relative amount of *trans*-enamine formed by either E166A or wild-type SHV-1, the 1696 cm<sup>-1</sup> stretch of the C2 ketone can serve as an internal standard (see species F in Table 4). This moiety is common to all clavulanate acyl-enzymes following opening of the oxazolidinium ring. Peak intensity ratios of the *trans*-enamine stretch to the carbonyl stretch are approximately 10 in E166A and 3 in the wild type. These intensities suggest that clavulanate forms a predominant population of *trans*-enamine with E166A but only a fraction of *trans*-enamine with wild-type SHV-1. The identities of the other acyl-enzymes are discussed below.

Clavulanate generates a minor population of *cis*-enamine with both enzymes. Like sulbactam, the 1585 cm<sup>-1</sup> shoulder features of both difference spectra in Figure 5 are assigned to the *cis*-O=C–C=C–NH– stretch (Table 3 and Figure 5). While a crystal structure is not available for the clavulanate/SHV-1 complex, this intermediate was not detected in the clavulanate/E166A structure. Its absence is attributed to two factors: (1) The *cis*-enamine is a minor product in the reaction between clavulanate and E166A. Intermediates constituting less than 30% active-site occupancy are difficult to observe in X-ray crystallography. (2) Crystals of  $\beta$ -lactamase/inhibitor complexes are flash-cooled to 120 K after “soak-in”, and their structures are determined at cryogenic temperatures. Compared to Raman crystallography, where the spectra are recorded at room temperature, the colder temperature used in X-ray analysis favors the more enthalpically stable *trans*-enamine species.

Peaks at 1662 and 1647 cm<sup>-1</sup> are assigned to a pair of imine acyl-enzymes (Figure 5, top). As demonstrated by the spectra, these intermediates are only made in appreciable amounts with the wild-type enzyme. More specifically, the 1662 cm<sup>-1</sup> band in the SHV-1/clavulanate complex is assigned to a C5=N4 imine (species 7, Scheme 3) that results from cleavage of the C–O bond and concomitant opening of the oxazolidinium ring. Structurally, this imine is analogous to those formed by sulbactam and tazobactam. Tautomerization of imine 7 to imine 8 in Scheme 3 is driven by resonance with the adjacent ketone



Scheme 3. Revised Reaction Scheme for Clavulanate in SHV-1<sup>a</sup>

<sup>a</sup> The N4=C5 imine is unique to clavulanate and a direct result of decarboxylation.

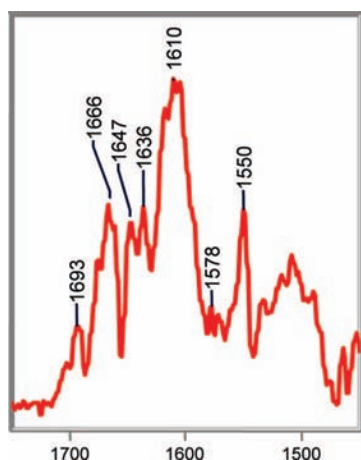


**Figure 6.** Partial Raman difference spectrum of the acyl-enzyme-derived intermediates from clavulanate with SHV-1 following reduction by sodium cyanoborohydride, a mild reducing agent that is specific for protonated imines.

at C2. The N4=C3 imine, which is marked by the 1647 cm<sup>-1</sup> band in the Raman spectrum, is unique to clavulanate and was first detected by mass spectrometry.<sup>37</sup> QM calculations on compounds **F** and **G**, which are models for the C5=N4 and N4=C3 imines, predict strong C=NH<sup>+</sup> stretching modes near 1663 and 1648 cm<sup>-1</sup>, respectively (Table 4). Lastly, the frequency of both the 1662 and 1647 cm<sup>-1</sup> species shifts down by approximately 20 cm<sup>-1</sup> in D<sub>2</sub>O due to NH/ND exchange, which further confirms their assignments (data not shown).

Until now, assignment of the imine features was based on their frequency in the Raman spectra, response to NH/ND exchange, and QM calculations. Here, we provide additional support for these assignments by chemical modification of the imine moiety using sodium cyanoborohydride, a mild reducing agent. In this experiment, a crystal of SHV-1 is soaked in a 5 mM bath of clavulanate for 20 min to allow for the maximum amount of acyl-enzyme to accumulate. Then the crystal complex is treated with a 2-fold excess of sodium cyanoborohydride. This reducing agent is less reactive than its parent compound, sodium borohydride, and is considered to react only with protonated imines and not with their unprotonated counterparts.<sup>38</sup> The relevant portion of the difference spectrum of the

clavulanate complex following treatment with sodium cyanoborohydride is shown in Figure 6. Although the O=C–C=C–NH– stretch of clavulanate's *trans*-enamine species is unaffected, the intensities of the 1662 and 1649 cm<sup>-1</sup> bands are markedly reduced, providing evidence they are associated with protonated imines.

## Conclusion

To design an effective inhibitor, it is necessary, as a starting point, to identify large populations of stable intermediates that are formed by mechanism-based inhibitors. Various pathways have been proposed for the inhibition of  $\beta$ -lactamases by mechanism-based inhibitors; however, all share the first two steps: (1) The active-site serine residue reacts with the carbonyl carbon atom to form a tetrahedral intermediate at the carbonyl carbon atom. (2) The C–N bond in the  $\beta$ -lactam ring is cleaved, and an acyl-enzyme is formed. Analysis of the resulting acyl-enzymes is complicated by the number of potential intermediates and branched reaction pathways. Extensive early studies via kinetics, X-ray analysis, and mass spectrometry provide a fragmented picture in which there are no integrated data showing which chemical species are present and providing information on their relative populations. There are only three crystallographic studies in the literature of complexes formed between wild-type  $\beta$ -lactamases and the clinical inhibitors. These studies underline the fact that a wide variety of intermediates, differing from enzyme to enzyme, can be detected by X-ray analysis. Consequently, there is no consistent message as to whether the *cis*- or *trans*-enamine, imine, or S130 adduct is responsible for inhibition on a relevant time scale. Moreover, studies which provide high-resolution X-ray data on stoichiometric complexes of enzyme and inhibitor often use a catalytically impaired form of the enzyme, i.e., E166A. Here, we show that it may be hazardous to employ a structure-based design based on the latter results as comparative studies on the wild-type enzyme reveal a much higher level of complexity. For instance, several intermediates are formed in the inactivation of SHV-1 by clavulanate. In distinction, only a single adduct, the *trans*-enamine, is found when E166A  $\beta$ -lactamase is inactivated by clavulanate under the same conditions. One notable exception is tazobactam, which forms a predominant population of *trans*-enamine with both the wild type and E166A. The ability of tazobactam to form a stable population of *trans*-enamine, even

(37) Sulton, D.; Pagan-Rodriguez, D.; Zhou, X.; Liu, Y.; Hujer, A. M.; Bethel, C. R.; Helfand, M. S.; Thomson, J. M.; Anderson, V. E.; Buynak, J. D.; Ng, L. M.; Bonomo, R. A. *J. Biol. Chem.* **2005**, *280* (42), 35528–36.

(38) Borch, R. F.; Bernstein, M. D.; Durst, H. D. *J. Am. Chem. Soc.* **1971**, *93* (12), 2897–2904.

in the wild-type background, explains its superior performance in both enzyme- and cell-based assays. This ability is directly associated with the triazole group of tazobactam, which provides for hydrogen-bonding and hydrophobic interactions with the enzyme. The *trans*-enamine forms of sulbactam and clavulanate do not exploit any protein/ligand interactions in the “tail” of the molecule. Therefore, one approach to design more effective mechanism-based compounds is to increase the complexity and diversity of C2 substituents of penam sulfone and clavam scaffolds. These compounds must then be evaluated on their ability to form stable *trans*-enamine populations.

**Acknowledgment.** National Institutes of Health Grant RO1 GM54072 (P.R.C.), the Case Western Reserve University MSTP

Program (M.K.), and Robert A. Welch Foundation Grant N-0871 (J.D.B.) supported this study. We are grateful to Dr. V. E. Anderson for his suggestion that sodium cyanoborohydride is a reducing agent specific for protonated imines.

**Supporting Information Available:** Raman difference spectra of the tazobactam/SHV E166A complex in H<sub>2</sub>O at room temperature, Raman difference spectra of the tazobactam/SHV S130G complex in H<sub>2</sub>O at room temperature, and complete ref 32. This material is available free of charge via the Internet at <http://pubs.acs.org>.

JA808311S